Placenta 168 (2025) 135–143

Contents lists available at ScienceDirect

Placenta

journal homepage: www.elsevier.com/locate/placenta

Patterns of trophoblast migration in deep uterine arteries in accreta placentation

Anna Allen [a], Carolyn J.P. Jones [a], Eric Jauniaux [b], Ahmed Hussein [c], John D. Aplin [a,*]

[a] Maternal and Fetal Health Research Centre, Division of Developmental Biology & Medicine, School of Medical Sciences, Faculty of Biology, Medicine and Health, University of Manchester, Central Manchester University Hospital NHS Foundation Trust, Manchester Academic Health Sciences Centre, St Mary's Hospital, Oxford Road, Manchester, M13 9WL, UK

[b] Institute for Women's Health, Faculty of Population Health Sciences, University College London (UCL), London, UK

[c] Department of Obstetrics and Gynaecology, Faculty of Medicine, Kasr Al-Ainy, University of Cairo, Egypt

ARTICLE INFO

Keywords:
Placenta accreta spectrum
Histopathology
Extravillous trophoblast
Artery remodelling
Inflammatory cells

ABSTRACT

Introduction: During normal placentation, extravillous trophoblast (EVT) colonises and, in synergy with maternal leukocytes, transforms the walls of uterine spiral arteries in the decidua and inner myometrium. In placenta accreta spectrum (PAS), migration of extravillous trophoblasts (EVT) is abnormally deep, reaching larger upstream arteries in myometrium. As little is known about their interactions in accreta areas, scar tissue and deeper arteries were examined for colonisation and remodelling by trophoblast and maternal inflammatory cells.

Methods: Samples (n = 79) were fresh hysterectomy specimens taken immediately after surgery in 11 patients presenting with placenta previa accreta at birth, at term or near term. They were obtained from accreta areas, non-accreta areas and, in cases of associated dehiscence of the lower uterine segment, from the adjacent shell (uterine boundary membrane). Samples were stained using antibodies to EVT (cytokeratin) or inflammatory cells (CD45). Arterial profiles positioned within 5 mm of villous placenta at scar sites were included in the analysis (54 lumina).

Results: EVT colonisation of scar tissue was much more extensive than in adjacent myometrium ($p < 0.001$). Large arteries were remodelled (20.3 %), partially remodelled (22.2 %) or unremodelled (29.6 %). Unremodelled arteries were present in 10/11 specimens while 6/11 had one or more fully remodelled. Leucocytes/inflammatory cells were frequently associated with arteries undergoing remodelling. EVT also accumulated beneath the serosa but were not found to cross it.

Discussion: Some remodelling of deep arteries occurs in most samples from accreta areas, but persistence of unremodelled arteries in distal segments with abnormally high velocity intraplacental blood flow is probably the main mechanism leading to lacuna formation.

1. Introduction

Placenta accreta is defined by the abnormal attachment of one or more placental cotyledons to the uterine wall at birth [1–3]. With rapid increases in cesarean delivery (CD) rates, more than 90 % of cases of placenta accreta spectrum (PAS) are found in patients with a history of lower uterine segment (LUS) cesarean section presenting with an anterior low-lying placenta or placenta previa [4,5]. Although accreta placentation has been described in association with a scar of the upper uterine segment (non-previa accreta), or a congenital uterine anomaly, or uterine pathologies such as adenomyosis (accreta in an unscarred uterus), these cases are rare and poorly documented clinically and histologically [1,4].

Patients with a history of CD, especially those with prior multiple CDs, often have a large cesarean scar defect (CSD) or niche of the LUS and, in subsequent pregnancies, are at high risk of cesarean scar ectopic pregnancies (CSEP) [6], half of which when ongoing will develop into a placenta previa accreta [7–9]. The residual niche comprises scar tissue incorporating disorganised myocyte layers with fibrosis, tissue edema, inflammation and elastosis covered by an atrophic endometrium [10]. In normal gestation, trophoblast escaping from the tips of anchoring villi (extravillous trophoblast, EVT) in the first and second trimester migrate through the decidua to the junctional zone, and a smaller population of cells progresses further into the inner third of the myometrium. The

* Corresponding author. Maternal and Fetal Health Research Centre, St Mary's Hospital, Oxford Road, Manchester, M13 9WL, UK.
E-mail address: john.aplin@manchester.ac.uk (J.D. Aplin).

https://doi.org/10.1016/j.placenta.2025.06.014
Received 19 March 2025; Received in revised form 31 May 2025; Accepted 22 June 2025
Available online 24 June 2025

walls of spiral arteries in these areas are populated and transformed to create passive (non-contractile) channels by cooperative action of EVT and maternal inflammatory cells [11–13]. In accreta placentation, there is evidence of extensive EVT migration reaching deeper layers of the myometrium and the corresponding larger arteries (radial and arcuate) [14–19]. In PAS, both the development of villous tissue inside a scar and the abnormally deep EVT are associated with major changes in the utero-placental and intraplacental circulation on ultrasound imaging and at birth [8,18–20].

Understanding placentation in PAS requires an integrative view of how the placental/scar interface is established, colonisation of maternal tissue by EVT and subsequent growth of the villous tree [9]. Recent findings show that the scar may strongly influence patterns of EVT migration [21] and suggest that arterial wall remodelling in deeper sites, analogous to that of spiral arteries, might allow local expansion of vessel openings, thus mitigating the impact of high velocity flow. The aim of this study was to examine the susceptibility of both scar tissue and deeper arteries to colonisation and remodelling by EVT and maternal inflammatory cells and to examine the behaviour of EVT that reaches the uterine wall. The novelty of the work resides in the analysis of multiple biopsies taken at different depths in the uterine scar in fresh hysterectomy specimens from pregnancies complicated by PAS, evaluation of changes to deep uterine arteries arising nearby scar areas heavily colonised by trophoblast, and our insights into the distinct behaviour of extravillous trophoblast in scar tissue, myometrium and when it reaches the subserosal surface layer of the uterus.

2. Materials and methods

2.1. Study design

This was a retrospective analysis of prospectively collected data from 11 patients diagnosed with PAS at birth who had an elective near-term cesarean hysterectomy in the Department of Obstetrics and Gynecology, University of Cairo, Egypt [22]. All patients had a history of ≥2 prior CDs and presented with an anterior placenta previa on transabdominal and transvaginal scan (TVS). The diagnosis of PAS at birth was confirmed when one or more placental cotyledon(s) could not be digitally separated from the uterine wall at delivery or during the gross examination of the fresh hysterectomy specimens as previously described [22].

Detailed transabdominal sonographic and TVS examinations including color Doppler imaging (CDI) mapping of the placenta and utero-placental interface (GE Voluson E10, GE Medical System, Zipf, Austria) were performed within the 48 h that preceded surgery. Ultrasound findings were recorded using a standardized protocol including anomalies of uterine contour (loss of clear zone, myometrial thinning and placental bulge) and anomalies of the utero-placental, intraplacental and cervical circulation [23]. Lacunae were also recorded according to the score proposed by Finberg and Williams [24] i.e. 0 = none, 1+ = 1–3, 2+ = 4–6, 3+ = >6.

Ethical committee approval was obtained before the start of the study (Institutional Scientific and Research Ethical Committee approval at the University of Cairo (RSEC 021001)). All participants gave their informed consent after a detailed explanation of the study's purpose. All data were fully anonymised before analysis.

2.2. Histopathologic examination

Tissue blocks were obtained from fresh hysterectomy specimens as previously described [22]. In all cases, samples including the whole thickness of uterine wall, the placental bed and at least a third of the placental thickness were collected from accreta areas and areas with no gross evidence of abnormal placental attachment. Samples were also collected in six cases from the uterine margin adjacent to the dehiscence area. A total of 79 samples were obtained (averaging about 7 per patient and taken at advancing depth up to and including the serosa) and fixed in 10 % neutral buffered formalin, wax embedded and sections stained with hematoxylin and eosin (H&E).

2.3. Immunohistochemistry

Sections 5μm thick were dewaxed, then stained for cytokeratin 18 (CK18, C8541, Clone CY-90, Sigma Aldrich, Dorset, UK), leucocytes (CD45, common leukocyte antigen Clone 2B11 + PD7/26, DAKO, California, USA) and desmin (polyclonal, Stratech, Ely, UK). The desmin antibody required antigen retrieval with a citrate buffer at pH 6.0. Endogenous peroxidases were quenched by incubation for 10 min with 3 % hydrogen peroxidase (VWR Chemicals, Leicestershire, UK) and after TBS washes were treated to prevent non-specific binding (goat serum (G9023, Sigma Aldrich, Dorset, UK), human serum (H4522, Sigma Aldrich) and Tween 0.1 % in TBS) for 30 min. Incubation in the primary antibody (CK18 1:500, CD45 1:200 and Desmin 1:200) was carried out overnight at 4 °C. Slides were washed with TBS/Tween and goat anti-mouse (16729-AAT, Stratech, Cambridge, UK; 1:300) was applied for 30 min followed by TBS washes and incubation in avidin-peroxidase (A3151, Sigma Aldrich, Dorset, UK; 1:200) for 30 min. Binding was revealed by treatment with 3,3-diaminobenzidine (DAB) (SK-4100, Vector Laboratories, Newark, California, USA) then slides were washed, briefly counterstained in Modified Mayer's Hematoxylin and mounted in DePeX. Some sections stained for cytokeratin were counterstained with both hematoxylin and eosin before dehydration and clearing. All sections were digitised for archiving (SlideScanner, 3D Histech Panoramic 250) and analysed using SlideViewer Software (Version 2.6, 3DHISTECH Fejlesztő Korlátolt Felelősségű Társaság (3DHISTECH Kft.).

2.4. Analysis of extravillous trophoblasts in scar tissue and myometrium

Slides stained for the muscle marker desmin were used to distinguish myometrium from scar tissue in areas adjacent to the villi before further analysis of fibrinoid and EVT to avoid unconscious bias (not shown). The same areas were located on slides stained with CK18/H&E and an annotation square size 1500px x 1500px was added. A threshold for positive cell identification was then optimised and the cells in each square were counted and classified as positive or negative (Supplemental Fig. 1A–F, zoom into annotation boxes). The proportion of stained cells was exported into GraphPad Prism (Version 10.0.1, © 1994–2021 GraphPad Software, LLC) where the data were corrected using a ROUT outlier test, characterised using a D'Agostino and Pearson normality test and, where non-parametrically distributed, compared using a Mann-Whitney *U* test.

Samples (34) were excluded from this analysis if they had no villous placenta, no maternal scar tissue or myometrium, no maternal tissue along the placental-uterine interface, no maternal tissue that could be reliably identified, or if there were significant areas of tissue detachment. Ideally, samples had both myometrium and scar tissue measurements taken, however some contained only one tissue type.

2.5. Assessment of fibrinoid deposition in scar tissue and myometrium

Areas of scar tissue and myometrium adjacent to villi were first identified on desmin-stained slides and then annotation boxes (1500px x 1500px) were added to the corresponding areas of the CK18/H&E slides on QuPath. A pixel classifier was set up for fibrinoid detection and run for all annotation boxes. The data were imported into GraphPad Prism, checked for non-normality and compared using a Mann-Whitney *U* test. Exclusion criteria for this analysis were as above resulting in 55 exclusions.

2.6. Correlation between trophoblast and fibrinoid deposition in scar tissue

Scar tissue was identified on desmin-stained slides and matched to corresponding areas on the CK18/H&E-stained slides. A thick band of EVT in scar tissue adjacent to the villi was often found associated with areas of abnormal adhesion of villi, and its incidence was noted. CK18/H&E images were imported into QuPath and 5 annotation boxes each 1500px x 1500px were spaced apart equally along the area of abnormal adhesion (Supplemental Fig. 2A). One script was set up to count numbers of stained EVTs (Supplemental Fig. 2B) and another to make a pixel threshold to estimate amounts of fibrinoid deposition in each box (Supplemental Fig. 2C and D). All measurements were exported into GraphPad Prism. The relationships between variables did not differ significantly from linearity, and variables were approximately normally distributed, so a Pearson's correlation coefficient was used. Excluded samples (28) included those with a lack of villi, lack of scar tissue and sections impaired by significant areas of tissue detachment from the slide.

2.7. Evaluation of the extent of remodelling of arteries in the myometrium

Using C18 K/H&E-stained slides, all arterial lumens within 5 mm of the intervillous space, excluding embedded villi, were identified as either: 1) unremodelled, 2) unremodelled but with at least 1 EVT cell in the arterial wall, 3) partially remodelled, 4) fully remodelled, 5) displaying intimal hyperplasia with remodelling or 6) intimal hyperplasia without remodelling. The location of each artery was also noted i.e. scar, myometrium, stroma or fibrinoid.

The criteria for remodelling were: fibrinoid deposition around the vessel wall, EVTs invading the wall, disruption or absence of smooth muscle and the presence of inflammatory cells. An artery with all 4 was classed as fully remodelled, while those with 1–3 were classed as partially remodelled. Intimal hyperplasia was defined as a deposition of connective tissue cells within the inner arterial wall.

3. Results

All patients had an anterior placenta previa reaching or covering the cervix and were delivered at or near term (36–37 weeks) (Table 1). They presented on pre-operative ultrasound examination with major dehiscence of the LUS, placental bulging (part of the placenta herniated through the dehiscence) hypervascularisation of the utero-placenta interface and a lacuna score >2 and required a hysterectomy to control intraoperative bleeding. In all cases, around 10–15 % of the placental basal plate was found to be abnormally attached to the uterine wall.

3.1. Interface characteristics and patterns of EVT colonisation of scar and myometrium

Scar tissue was characterised by prominent large anisotropically-distributed collagen fibrils (Fig. 1A) and lacked immunostaining for desmin, which marks myometrium (not shown). Cytokeratin immunostaining revealed extensive colonisation of scar tissue by EVT (Fig. 1B), with significantly fewer cell numbers in myometrium (Fig. 3C; $p < 0.001$) where they largely occurred as widely spaced single cells or small groups, suggesting a preference for migration within the scar tracts.

Extensive and thick fibrinoid deposition was apparent at the villus-scar interface, more associated with scar than with myometrium ($p = 0.0031$) (Fig. 2A). Often EVT cells formed dense bands within the scar, especially where villi were attached to fibrinoid superficial to scar tissue (Table 2). The EVT count in the band and amount of fibrinoid deposited in the same area were highly correlated ($p < 0.0001$) (Fig. 2B). The results plotted by both biopsy site and patient number show that this trend is present with both variables (Fig. 2C), indicating the amount of fibrinoid and incidence of EVT are correlated, both per biopsy and per patient.

Table 1
Clinical characteristics of the 11 women included in the sample set. Lacunae were graded as proposed by Finberg and Williams [20]: 0 = none, 1+ = 1–3, 2+ = 4–6, 3+ = >6. Y = Years, CS = Cesarean section, wks = weeks, g = grams, IQR = Interquartile range.

Variables	Median (IQR)
Age (y)	35 (32–28)
Gravidity	6 (5–6)
Parity	4 (3–5)
Number of previous CS's	3 (3–4)
Gestation age at delivery (wks)	37 + 3 (36–37)
Fetal weight (g)	2850 (2760–2975)
Ultrasounds	**n (%)**
Loss of clear zone	
Yes	11 (100)
No	0 (0)
Bladder wall interruption	
Yes	0 (0)
No	11 (100)
Placental bulge	
Yes	7 (63.6)
No	4 (36.4)
Lacunae:	
1+	3 (27.3)
2+	3 (27.3)
3+	5 (45.5)
Intraoperative gross	**n (%)**
Size of dehiscence	
Moderate	2 (18.2)
Major	9 (81.8)
Placental bulge	
Yes	9 (81.8)
No	2 (18.2)

There was no correlation between the number of EVTs and the number of previous CDs ($p = 0.7419$), nor between the amount of fibrinoid deposition and the number of previous CDs ($p = 0.7599$). There was also no correlation between the amount of fibrinoid deposition and fetal weight ($p = 0.5054$).

3.2. Arterial wall transformation with loss of vascular smooth muscle can occur in deep arteries in association with EVT

Large patent arteries were present adjacent to the myometrium/scar boundary (Fig. 3). In some cases, arterial profiles were incorporated into fields of scar tissue and even opened into the intervillous space (IVS) (Fig. 3). There were 54 arterial lumina found in scar tissue or myometrium within 5 mm of villous placenta; some were unremodelled but had at least 1 intramural EVT (5.6 %). Others were remodelled (20.4 %), partially remodelled (22.2 %) or unremodelled (29.6 %), with some arterial sections, including those situated near the IVS, completely lacking intramural EVT. Overall, EVT was present in 61 % of arterial profiles located within 5 mm of villous placenta (Table 3). Where EVT was absent, arterial profiles were not conspicuously remodelled, but other arteries containing abundant mural EVT showed remodelling largely consistent with that seen in spiral arteries in normal pregnancy, ranging from focal muscle layer disruption to full replacement of smooth muscle with fibrinoid, and embedding of large EVT cells within the wall (Fig. 4A). Some arterial walls contained EVT despite the absence of local interstitial EVT, consistent with possible counter-current intramural migration (Fig. 4D).

Inflammatory cells were commonly seen in adventitial and mural regions of both remodelled and unremodelled arterial profiles (Figs. 4B and. 5C,D), with no obvious correlation with the degree of mural remodelling. Intimal hyperplasia was quite common in the presence and absence of both EVT and $CD45^+$ cells (Figs. 4 and 5), especially in

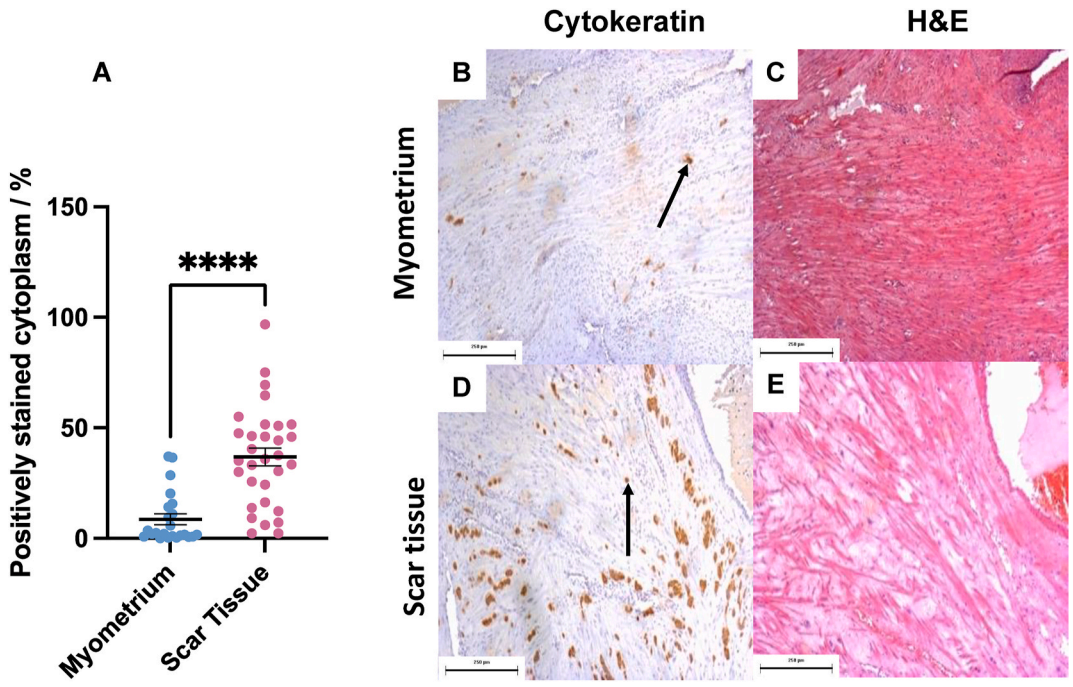

Fig. 1. There are more EVTs in scar tissue than in myometrium. A) The proportion of EVT in the scar tissue vs the myometrium. A ROUT test (Q = 5 %) found 5 outliers in the myometrium group ($p < 0.0001$; Mann-Whitney *U* test). B) An area of myometrium containing EVTs (CK18; arrow). C) Adjacent section (H&E) showing the organised muscle fibres in myometrium. D) An area of scar tissue containing EVT (arrow). Note the increased number of EVTs compared to the myometrium. E) Adjacent section with H&E stain showing anisotropic collagen fibres characteristic of scar tissue. All areas imaged were adjacent to villous placenta (4x).

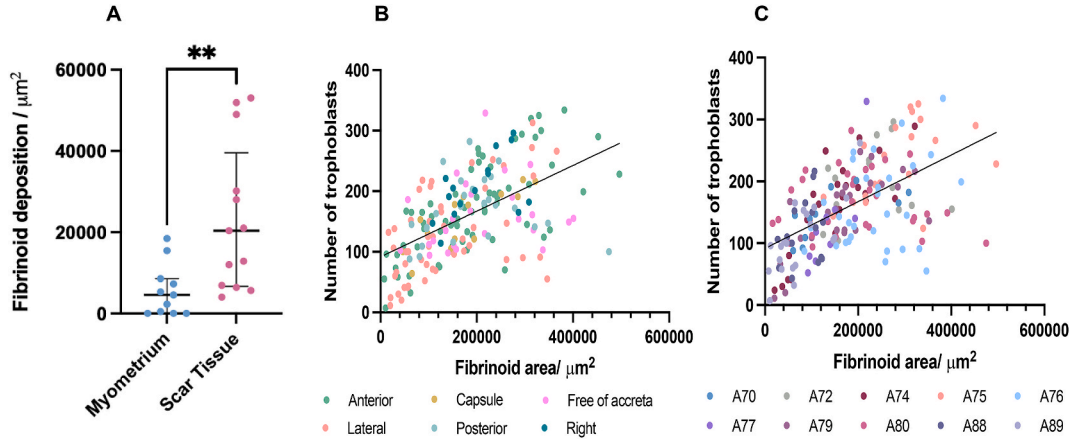

Fig. 2. A) There is more fibrinoid deposition in scar tissue (n = 13) than in myometrium (n = 11). Fibrinoid deposition in association with scar tissue exceeds that in myometrium ($p = 0.0031$**; Mann-Whitney *U* test; median ± IQR). B,C) EVT numbers are correlated with the amount of fibrinoid. B) A significant Pearson's correlation between the number of extravillous trophoblasts (EVT) and the amount of fibrinoid deposited in the extravillous trophoblast band adjacent to the villi ($p < 0.0001$), organised by biopsy site: anterior ($p < 0.0001$, n = 70), shell ($p = 0.0004$, n = 15), free of accreta ($p < 0.0001$, n = 50), lateral ($p = 0.2857$, n = 25), posterior ($p = 0.6765$, n = 25), right ($p = 0.0395$, n = 15). C) A significant Pearson's correlation between the number of EVTs and the amount of fibrinoid deposited in the extravillous trophoblast band adjacent to the villi, organised by patient number: A70 ($p = 0.032$, n = 10), A72 ($p = 0.51$, n = 15), A74 ($p < 0.0001$, n = 25), A75 ($p = 0.024$, n = 20), A76 ($p = 0.079$, n = 30), A77 ($p = 0.012$, n = 10), A79 ($p = 0.0001$, n = 25), A80 ($p = 0.84$, n = 30), A88 ($p = 0.339$, n = 15), A89 ($p = 0.0002$, n = 20). The black line indicates the positive correlation.

arterial segments close to the IVS. No other pathological changes were observed.

3.3. *The serosa limits the migration of extravillous trophoblasts*

Fig. 6 shows an example of one of two observed sites where EVT had migrated through the entire thickness of the myometrium, resulting in a thick band of cells adjacent to the submesothelial collagen layer under the serosal mesothelium covering the dehiscence shell. No EVT cells were found to cross this layer.

4. Discussion

Our data show that migration of EVT into and within scar tissue under accreta areas is much more efficient than into adjacent myometrium in which the layering of adjacent muscle cells remains intact. Deep myometrial arteries can be colonised by EVT and transformed similarly to spiral arteries in the normal placental bed. Numbers of Ki67-positive

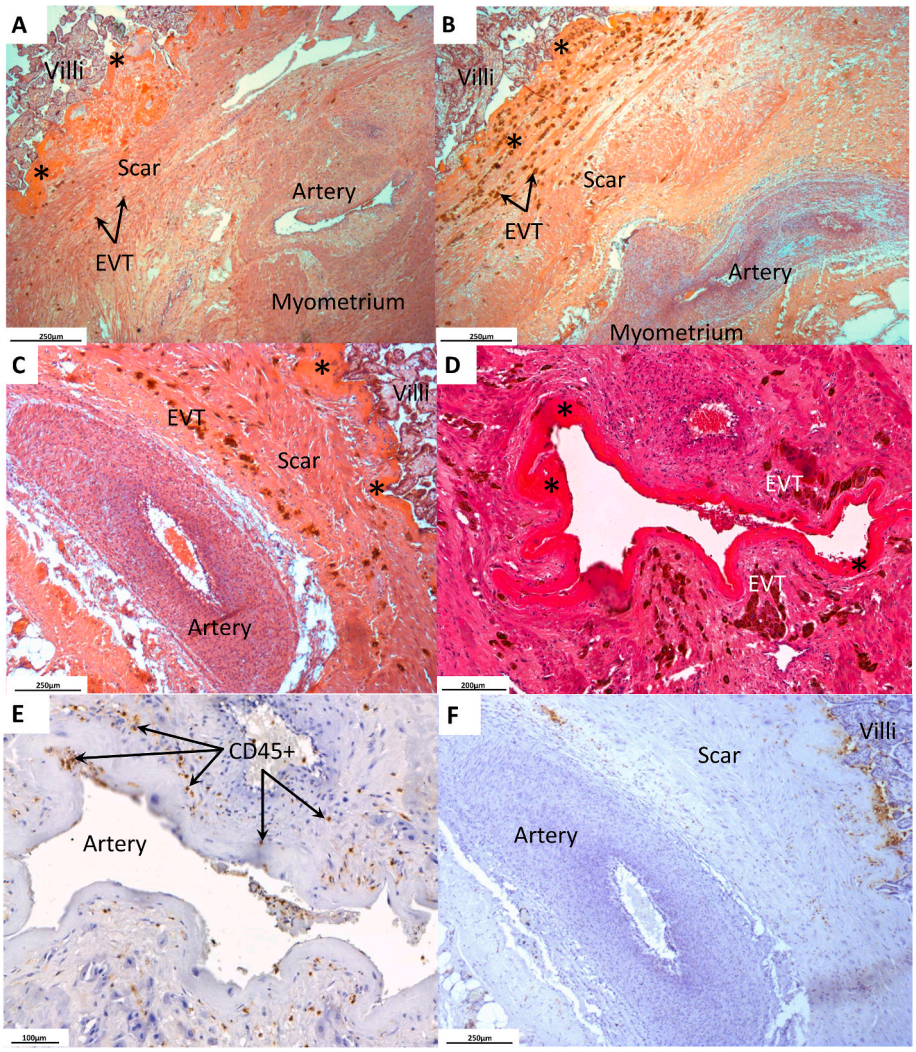

Fig. 3. A-C) Large patent arteries are found adjacent to the myometrium/scar boundary. CK18/H&E staining showing arterial profiles near the IVS completely lacking mural colonisation despite the nearby presence of interstitial EVT (arrows). Fibrinoid abuts the placental villi (*). D) Typically irregular transformed arterial profile with CK + EVT, loss of smooth muscle and deposition of fibrinoid (*) with replacement of the normal wall. E) A transformed artery containing mural and adventitial brown-staining $CD45^{+}$ cells. F) An unremodelled artery lacking $CD45^{+}$ cells. It also lacks EVT. (For interpretation of the references to color in this figure legend, the reader is referred to the Web version of this article.)

interstitial EVT in accreta cases at term are no different from EVT in control placental beds [15,16] but near-term EVT have largely left the cell cycle, thereforestudies in early gestation are required to address proliferative behaviour in scar environments.

Several authors [25–27] have suggested that EVT in PAS may be inherently more invasive than in normal pregnancy, akin to a trophoblastic cancer phenotype. However, candidate proteins have been identified in villous tissue rather than in EVT, and functional studies have been carried out either in trophoblast cell lines [25,26] or in one case [27] villous cytotrophoblast isolated from later gestation PAS. By analogy with normal placental development, the colonisation of scar tissue by EVT would be expected to occur largely in the first half of pregnancy. In these studies, there is no detailed description on the intraoperative and histopathologic findings and/or insufficient information about the area(s) of the utero-placental interface from which samples were obtained. All our samples were obtained from accreta areas in fresh hysterectomy specimens [22], and thus should provide an accurate evaluation of EVT migration under abnormally attached villous tissue.

An alternative hypothesis is that distinct uterine tissue environments regulate gene expression and migratory behaviour in trophoblast, as inferred from the greater abundance of EVT in scar environments than in closely adjacent myometrium seen in the present data and reported by others [14–19,27]. It is also pertinent that EVT cells in tubal pregnancies show more proliferative and invasive characteristics than their intrauterine counterparts [28,29]. Finally, we have shown that EVT migration is completely blocked by the collagenous layer beneath the serosa, suggesting that the densely packed collagen fibrils can resist penetration by EVT. Though we cannot formally rule out an inherited predisposition to more aggressive EVT colonisation of the scar in PAS patients, data here are consistent with accreta placentation arising via the loss in the scar area of physiological mechanisms arising from the maternal decidual and superficial myometrium environment that normally regulate EVT migration.

Large arcuate and radial arteries are present [30] in the deep myometrium, and arterial segments can become incorporated into scar fields during the remodelling of the LUS after CD. Unlike in normal unscarred uterine wall, where only the (more superficial) spiral arteries are accessed [11,12], placental growth into the scar makes the arcuate and radial arteries accessible to the migrating EVT population. When larger diameter arteries open into the intervillous space, high-velocity flow of blood may displace villi, creating lacunae in ultrasound images and

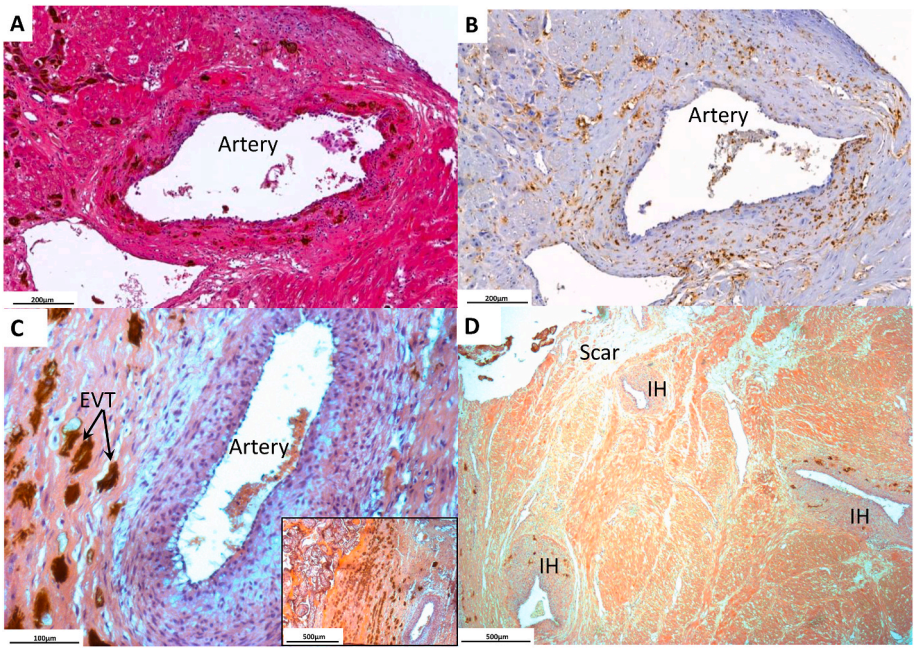

Fig. 4. A,B) A remodelled vessel with CD45^{+} inflammatory cells and CK18+ EVT in the wall. Serial sections stained with A) H&E/CK18 showing EVT and B) CD45 showing inflammatory cells stained brown. C) Intimal hyperplasia with mural disruption is seen in the absence of mural EVT despite the presence of nearby CK18+ EVT in scar tissue. The intervillous space (IVS) is ~1 mm to the left (inset). D) Intimal hyperplasia in the presence of darkly stained mural CK18+ EVT, seen in two arterial segments near scar tissue. (For interpretation of the references to color in this figure legend, the reader is referred to the Web version of this article.)

Table 2
A The number of samples from each patient containing an Extravillous Trophoblast (EVT) band directly adjacent to abnormally adhesive villi in scar tissue.

Patient number	EVT band and abnormal adhesion
A70	2/6
A72	3/5
A74	5/5
A75	5/5
A76	6/6
A77	3/3
A79	5/5
A80	6/7
A81	0/0
A88	4/4
A89	4/5

B The number of samples from each biopsy area containing an EVT band and abnormally adhesive villi.

Anterior	15/17
Capsule	3/8
Free of accreta	11/12
Lateral	5/5
Posterior	5/5
Right	4/4

raising the likelihood of shear stress and oxidative damage [18,23]. As the conceptus grows, the tissue containing large vessels thins so that, by term, the placenta may be covered by a semi-transparent vascularised membrane [31].

We analysed sites adjacent to large patent arteries where EVT colonisation had occurred and showed remodelling changes in almost two-thirds of those examined. Results may suggest that arcuate and radial arteries are less susceptible to remodelling than spiral arterial segments, but with the important caveat that, as EVT are fed into the placental bed from anchoring villi, the extent of their migration is likely to vary depending on the stage of early pregnancy at which anchoring sites formed within the adjacent scar and the remaining myometrial thickness. However, the variation between patients is significant; some of this can be ascribed to sampling that is, the likelihood of a given biopsy site containing a large artery. More studies will be required to allow correlation between implantation sites and scarred areas, and whether/when scar tissue and large arteries may be encountered by migrating EVT. Intraplacental tropism (adherent versus non-adherent sites in the same placenta) has been suggested to be driven by endothelial and stromal cells with notable differences in bone morphogenic protein 5 (BMP5) and osteopontin (SPP1) in the adherent vs nonadherent sites of placenta accreta spectrum [21], and certainly further work is required to advance understanding of abnormal adhesion.

Adherent villi within a prior cesarean scar tissue field produce large numbers of EVT which migrate freely within the scar, with a limited ability to penetrate into adjacent myometrium. Although it is difficult to track the level of proliferative activity in this population as gestation proceeds, normally in the placental bed proliferation slows in the second trimester and ceases altogether by 22 weeks. If this is so in the context of PAS, the extent of EVT colonisation of scar tissue and adjacent myometrium will depend on when the villous tissue encountered the scar site. An early encounter might lead to more abundant cells and deeper migration. Extensive fibrinoid deposition at the villus–scar interface [9] may contribute a provisional substrate to the formation of columns in first or second trimester that in turn give rise to the migratory population.

Deep myometrial arteries can be receptive to EVT colonisation and become transformed in a manner similar to spiral arteries in the normal placental bed. Leukocyte recruitment to the secretory phase endometrium is affected by scar tissue [32]; in the present study though maternal inflammatory cells were present in and around arterial walls, there was no simple correlation with EVT. Some deep vessels either resist remodelling (EVT in the vicinity have not penetrated the vessel wall) or are not reached by migrating EVT. Absence of mural remodelling is sometimes combined with channel constriction resulting from intimal hyperplasia and may cause blood from large arteries to enter the IVS at increased velocity.

Ultimately, where EVT cells reach the outer boundary of the uterus, migration is restricted by the outer thick collagenous shell, providing further evidence that colonisation of maternal tissue spaces is regulated

Table 3
Location of EVT within arterial media. EVT is present in the media of 61 % of arterial profiles located within 5 mm of the villous placenta. The different arterial patterns are listed by patient number. 33/54 profiles show some degree of remodelling with mural EVT present. These arteries are partially or fully remodelled with loss of vascular smooth muscle.

Sample	EVTs near unremodelled	Remodelled	Partially remodelled	Unremodelled	Intimal hyperplasia without remodelling	Intimal hyperplasia with remodelling	% with remodelling
A70			1	1	1		33
A72		4	4	1		1	90
A74		1		2		1	50
A75			1	1			50
A76		1	1	2		4	75
A77				2	1		0
A79	1			2			0
A80	1	2	2	1		2	86
A81							
A88		1	2	3		2	63
A89	1	2	1	1			75
Total:	3	11	12	16	2	10	

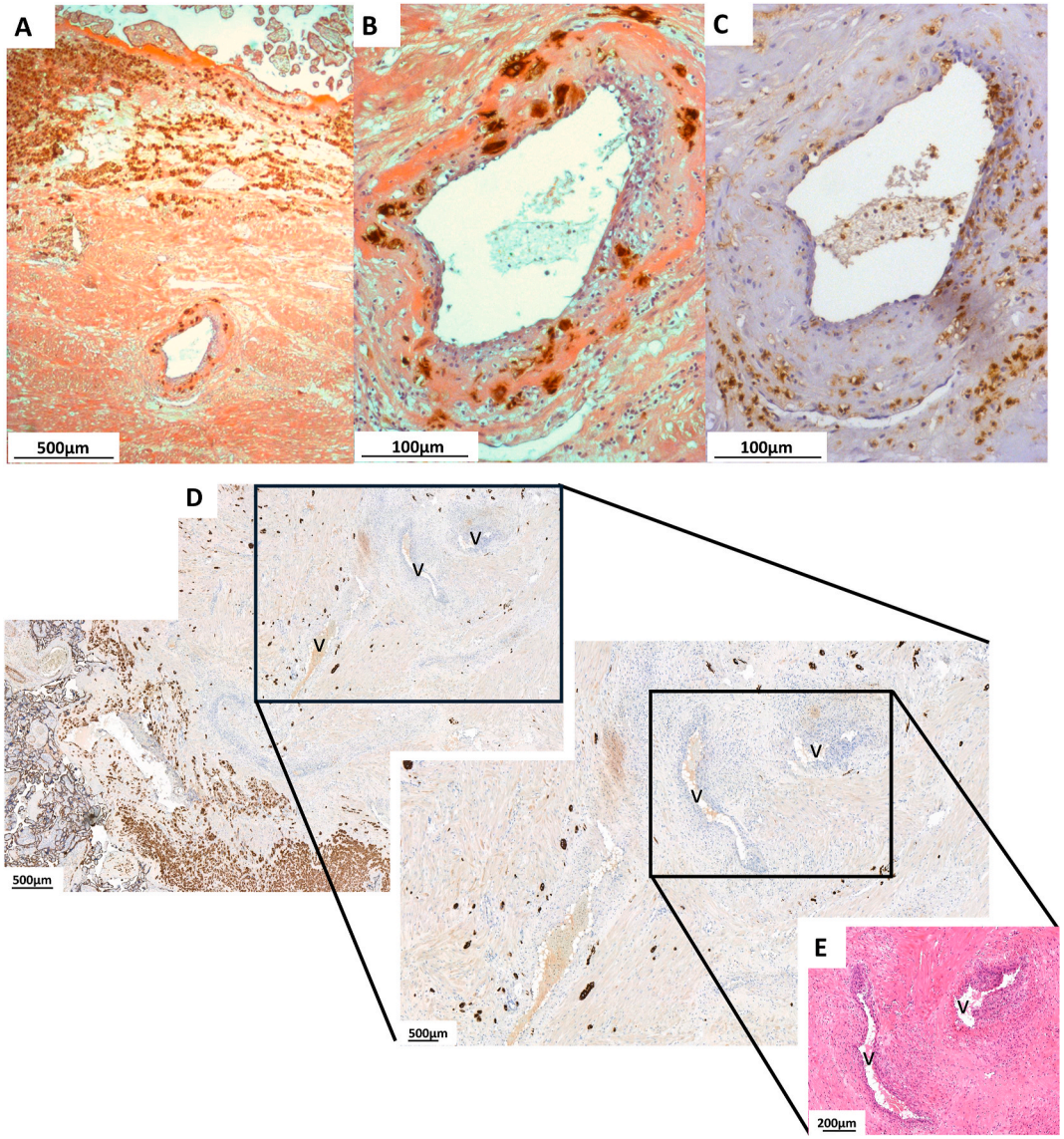

Fig. 5. A) and B) show CK 18+ mural EVT in an artery at low (A) and high (B) power, C) shows $CD45^{+}$ cells in the same vessel. D,E) Intimal hyperplasia in a vessel (v) crossing a field comprising mainly scar tissue towards the IVS, seen at bottom left. Note the absence of mural EVT, though interstitial EVT is present. D) CK18+ EVT cells enlarged in inset. E) H&E to show the structure of the vessel. See counts in Table 2.

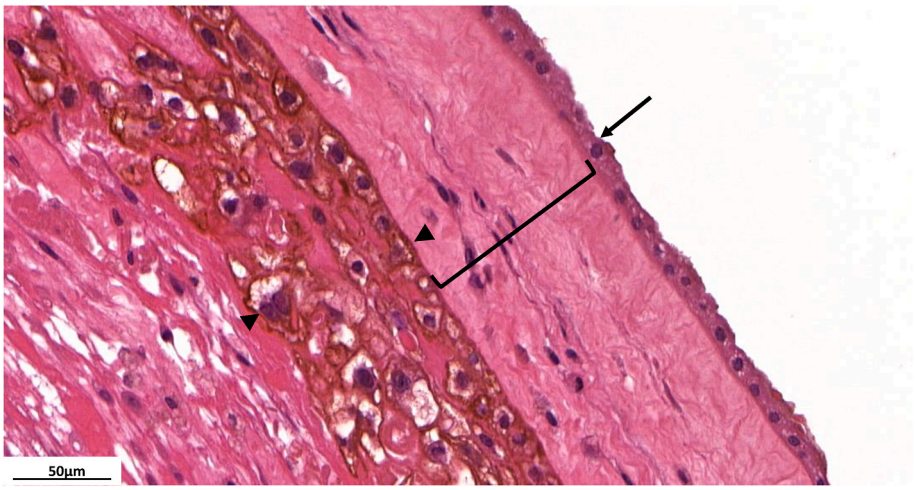

Fig. 6. Trophoblast layer near the serosa. Darkly stained extravillous trophoblasts can be seen in large numbers at the inner border of the surface connective tissue membrane (cytokeratin18/H&E). The arrow indicates mesothelium, an arrowhead indicates trophoblasts, the bracket indicates the collagenous layer.

by the very distinct mechanical, functional and biochemical properties of the various uterine layers.

5. Conclusion

Unregulated migration of EVT into and within scar tissue in PAS leads to colonisation of arcuate and radial arteries and transformation similar to spiral arteries in the normal uterine wall. Some deep vessels, however, resist remodelling – or the EVT may have arrived too late in pregnancy, given that migratory behaviour diminishes from late second trimester. This absence of mural remodelling combined with channel constriction resulting from intimal hyperplasia may cause jets of high-velocity maternal blood from large diameter arteries to enter the intervillous space, explaining the development of placental lacunae in accreta placentation. We can conclude that receptivity to EVT colonisation is not restricted to spiral arteries. We suggest that migration is altered by the maternal tissue environments colonised by EVT, previously characterised as 'loss of boundary limits' [19,21]. This will include the absence of physiological signalling and ECM arising from maternal decidual cells (including immune cells) that normally limit EVT migration, the more permissive environment of cesarean scar and the inherently more resistive properties of myometrium including in the area of scar dehiscence as the collagenous sub-serosa poses a barrier to their migration [33].

CRediT authorship contribution statement

Anna Allen: Writing – review & editing, Visualization, Methodology, Investigation, Formal analysis, Data curation. **Carolyn J.P. Jones:** Writing – review & editing, Visualization, Supervision, Methodology. **Eric Jauniaux:** Writing – review & editing, Resources, Investigation, Conceptualization. **Ahmed Hussein:** Writing – review & editing, Supervision, Resources, Methodology. **John D. Aplin:** Writing – review & editing, Writing – original draft, Visualization, Validation, Supervision, Resources, Project administration, Methodology, Investigation, Data curation, Conceptualization.

Funding statement

No funding external to the institutions involved was provided for this study.

Declaration of competing interest

The authors declare that they have no known competing financial interests or personal relationships that could have appeared to influence the work reported in this paper.

Acknowledgments

The authors wish to thank all the patients who donated tissue, and Frances Beards for histological and immunocytochemical expertise.

Appendix A. Supplementary data

Supplementary data to this article can be found online at https://doi.org/10.1016/j.placenta.2025.06.014.

References

[1] E. Jauniaux, D. Jurkovic, Placenta accreta: pathogenesis of a 20th century iatrogenic uterine disease, Placenta 33 (2012) 244–251, https://doi.org/10.1016/j.placenta.2011.11.010.
[2] Nijjar, S.; Jurkovic, D.; Hussein, A.M.; Jones, C.J.P.; Aplin, J.D.; Jauniaux, E., Evaluation of histopathologic changes associated with placentation in a cesarean section scar. Am. J. Obstet. Gynecol. ; in press.
[3] J.L. Hecht, R. Baergen, L.M. Ernst, P.J. Katzman, S.M. Jacques, E. Jauniaux, T. Y. Khong, L.A. Metlay, L. Poder, F. Qureshi, D.J. Roberts, S. Shainker, D.S. Heller Ds, Classification and reporting guidelines for the pathology diagnosis of placenta accreta spectrum (PAS) disorders: recommendations from an expert panel, Mod. Pathol. 33 (2020) 2382–2396, https://doi.org/10.1038/s41379-020-0569-1.
[4] E. Jauniaux, A. Bhide, Prenatal ultrasound diagnosis and outcome of placenta previa accreta after cesarean delivery: a systematic review and meta-analysis, Am. J. Obstet. Gynecol. 217 (2017) 27–36, https://doi.org/10.1016/j.ajog.2017.02.050.
[5] E. Jauniaux, F. Chantraine, R.M. Silver, J. Langhoff-Roos, FIGO Placenta Accreta Diagnosis and Management Expert Consensus Panel, FIGO consensus guidelines on Placenta accreta spectrum disorders: epidemiology, Int. J. Gynaecol. Obstet. 140 (2018) 265–273, https://doi.org/10.1002/ijgo.12407.
[6] S. Nijjar, E. Jauniaux, D. Jurkovic, Definition and diagnosis of cesarean scar ectopic pregnancies, Best Pract. Res. Clin. Obstet. Gynaecol. 89 (2023) 102360, https://doi.org/10.1016/j.bpobgyn.2023.102360.
[7] A.K. Agten, G. Cali, A. Monteagudo, J. Oviedo, J. Ramos, I. Timor-Tritsch, The clinical outcome of cesarean scar pregnancies implanted "on the scar" versus "in the niche", Am. J. Obstet. Gynecol. 216 (2017) 510.e1–510.e6, https://doi.org/10.1016/j.ajog.2017.01.019.
[8] E. Jauniaux, N. Zosmer, L.V. De Braud, G. Ashoor, J. Ross, D. Jurkovic, Development of the utero-placental circulation in cesarean scar pregnancies: a case-control study, Am. J. Obstet. Gynecol. 226 (2022) 399.e1–399.e10, https://doi.org/10.1016/j.ajog.2021.08.056.
[9] E. Jauniaux, D. Jurkovic, A.M. Hussein, G.J. Burton, New insights into the etiopathology of placenta accreta spectrum, Am. J. Obstet. Gynecol. 227 (2022) 384–391, https://doi.org/10.1016/j.ajog.2022.02.038.

[10] E. Debras, P. Capmas, C. Maudot, P. Chavatte-Palmer, Uterine wound healing after caesarean section: a systematic review, Eur. J. Obstet. Gynecol. Reprod. Biol. 296 (2024) 83–90, https://doi.org/10.1016/j.ejogrb.2024.02.045.
[11] R. Pijnenborg, L. Vercruysse, M. Hanssens, The uterine spiral arteries in human pregnancy: facts and controversies, Placenta 27 (2006) 939–958, https://doi.org/10.1016/j.placenta.2005.
[12] S.D. Smith, C.E. Dunk, J.D. Aplin, L.K. Harris, R.L. Jones, Evidence for immune cell involvement in decidual spiral arteriole remodelling in early human pregnancy, Am. J. Pathol. 174 (2009) 1959–1971, https://doi.org/10.2353/ajpath.2009.080995.
[13] J.D. Aplin, J.E. Myers, K. Timms, M. Westwood, Tracking placental development in health and disease, Nat. Rev. Endocrinol. 16 (2020) 479–494, https://doi.org/10.1038/s41574-020-0372-6.
[14] T.Y. Khong, W.B. Robertson, Placenta creta and placenta praevia creta, Placenta 8 (1987) 399–409.
[15] K.R. Kim, S.Y. Jun, J.Y. Kim, J.Y. Ro, Implantation site intermediate trophoblasts in placenta cretas, Mod. Pathol. 17 (2004) 1483–1490, https://doi.org/10.1038/modpathol.3800210.
[16] P. Tantbirojn, C.P. Crum, M.M. Parast, Pathophysiology of placenta creta: the role of decidua and extravillous trophoblast, Placenta 29 (2008) 639–645, https://doi.org/10.1016/j.placenta.2008.04.008.
[17] T. Hannon, B.A. Innes, G.E. Lash, J.N. Bulmer, S.C. Robson, Effects of local decidua on trophoblast invasion and spiral artery remodelling in focal placenta creta - an immunohistochemical study, Placenta 33 (2012) 998–1004, https://doi.org/10.1016/j.placenta.2012.09.004.
[18] E. Jauniaux, N. Zosmer, D. Subramanian, H. Shaikh, G.J. Burton, Ultrasound-histopathologic features of the utero-placental interface in placenta accreta spectrum, Placenta 97 (2020) 58–64, https://doi.org/10.1016/j.placenta.2020.05.011.
[19] E. Jauniaux, J.D. Aplin, K.A. Fox, Y. Afshar, A.M. Hussein, C.J.P. Jones, G. J. Burton, Placenta accreta spectrum, Nat. Rev. Dis. 11 (2025) 41. https://doi.org/10.1038/s41572-025-00628-z.
[20] E. Jauniaux, S. Collins, G.J. Burton, Placenta accreta spectrum: pathophysiology and evidence-based anatomy for prenatal ultrasound imaging, Am. J. Obstet. Gynecol. 218 (2018) 75–87.
[21] Y. Afshar, O. Yin, A. Jeong, G. Martinez, J. Kim, F. Ma, C. Jang, S. Tabatabaei, S. You, H.R. Tseng, Y. Zhu, D. Krakow, Placenta accreta spectrum disorder at single-cell resolution: a loss of boundary limits in the decidua and endothelium, Am. J. Obstet. Gynecol. 230 (2024) 443.e1–443.e18, https://doi.org/10.1016/j.ajog.2023.10.001.
[22] E. Jauniaux, A.M. Hussein, N. Zosmer, R.M. Elbarmelgy, R.A. Elbarmelgy, H. Shaikh, G.J. Burton, A new methodologic approach for clinico-pathologic correlations in invasive placenta previa accreta, Am. J. Obstet. Gynecol. 222 (2020) 379.e1–379.e11, https://doi.org/10.1016/j.ajog.2019.11.1246.
[23] E. Jauniaux, F. D'Antonio, A. Bhide, F. Prefumo, R.M. Silver, A.M. Hussein, S. A. Shainker, F. Chantraine, Z. Alfirevic, Modified Delphi study of ultrasound signs associated with placenta accreta spectrum, Ultrasound Obstet. Gynecol. 61 (2023) 518–525, https://doi.org/10.1002/uog.26155.
[24] H.J. Finberg, J.W. Williams, Placenta accreta: prospective sonographic diagnosis in patients with placenta previa and prior cesarean section, J. Ultrasound Med. 11 (1992) 333–343, https://doi.org/10.7863/jum.1992.11.7.333.
[25] R. Wang, W. Liu, J. Zhao, L. Liu, S. Li, Y. Duan, Y. Huo, Overexpressed LAMC2 promotes trophoblast over-invasion through the PI3K/Akt/MMP2/9 pathway in placenta accreta spectrum, J. Obstet. Gynaecol. Res. 49 (2023) 548–559, https://doi.org/10.1111/jog.15493.
[26] R. Wang, J. Zhao, C. Liu, S. Li, W. Liu, Q. Cao, Decreased AGGF1 facilitates the progression of placenta accreta spectrum via mediating the P53 signaling pathway under the regulation of miR-1296-5p, Reprod. Biol. 23 (2023) 100735, https://doi.org/10.1016/j.repbio.2023.100735.
[27] L. McNally, Y. Zhou, J.F. Robinson, G. Zhao, L.M. Chen, H. Chen, M.Y. Kim, M. Kapidzic, M. Gormley, R. Hannibal, S.J. Fisher, Up-regulated cytotrophoblast DOCK4 contributes to over-invasion in placenta accreta spectrum, Proc. Natl. Acad. Sci. USA 117 (2020) 15852–15861, https://doi.org/10.1073/pnas.1920776117.
[28] S. Randall, C.H. Buckley, H. Fox, Placentation in the fallopian tube, Int. J. Gynecol. Pathol. 6 (1987) 132–139.
[29] T. Gao, Y. Liang, H. Tang, L. Quan, The increased level of Tspan5 in villi suggests more proliferation and invasiveness of trophoblasts in tubal pregnancy, Eur. J. Obstet. Gynecol. Reprod. Biol. 228 (2018) 38–42, https://doi.org/10.1016/j.ejogrb.2018.05.033.
[30] G. Farrer-Brown, J.O. Beilby, M.H. Tarbit, The blood supply of the uterus. 1. Arterial vasculature, J. Obstet. Gynaecol. Br. Commonw. 77 (1970) 673–681.
[31] B.D. Einerson, J. Comstock, R.M. Silver, D.W. Branch, P.J. Woodward, A. Kennedy, Placenta Accreta spectrum disorder: uterine dehiscence, not placental invasion, Obstet. Gynecol. 135 (2020) 1104–1111, https://doi.org/10.1097/AOG.0000000000003793.
[32] J. Ben-Nagi, A. Walker, D. Jurkovic, J. Yazbek, J.D. Aplin, Effect of cesarean delivery on the endometrium, Int. J. Gynaecol. Obstet. 106 (2009) 30–34, https://doi.org/10.1016/j.ijgo.2009.02.019.
[33] E. Jauniaux, J.L. Hecht, R.A. Elbarmelgy, R.M. Elbarmelgy, M.M. Thabet, A. M. Hussein, Searching for placenta percreta: a prospective cohort and systematic review of case reports, Am. J. Obstet. Gynecol. 226 (2022) e1–837.e13, https://doi.org/10.1016/j.ajog.2021.12.030.